

4

Steady-State Electric and Magnetic Fields

A knowledge of electric and magnetic field distributions is required to determine the orbits of charged particles in beams. In this chapter, methods are reviewed for the calculation of fields produced by static charge and current distributions on external conductors. Static field calculations appear extensively in accelerator theory. Applications include electric fields in beam extractors and electrostatic accelerators, magnetic fields in bending magnets and spectrometers, and focusing forces of most lenses used for beam transport.

Slowly varying fields can be approximated by static field calculations. A criterion for the static approximation is that the time for light to cross a characteristic dimension of the system in question is short compared to the time scale for field variations. This is equivalent to the condition that connected conducting surfaces in the system are at the same potential. Inductive accelerators (such as the betatron) appear to violate this rule, since the accelerating fields (which may rise over many milliseconds) depend on time-varying magnetic flux. The contradiction is removed by noting that the velocity of light may be reduced by a factor of 100 in the inductive media used in these accelerators. Inductive accelerators are treated in Chapters 10 and 11. The study of rapidly varying vacuum electromagnetic fields in geometries appropriate to particle acceleration is deferred to Chapters 14 and 15.

The static form of the Maxwell equations in regions without charges or currents is reviewed in Section 4.1. In this case, the electrostatic potential is determined by a second-order differential equation, the Laplace equation. Magnetic fields can be determined from the same equation by defining a new quantity, the magnetic potential. Examples of numerical (Section 4.2) and analog

Steady State Electric and Magnetic Fields

(Section 4.3) methods for solving the Laplace equation are discussed. The numerical technique of successive overrelaxation is emphasized since it provides insight into the physical content of the Laplace equation. Static electric field calculations with field sources are treated in Section 4.4. The classification of charge is emphasized; a clear understanding of this classification is essential to avoid confusion when studying space charge and plasma effects in beams. The final sections treat the calculation of magnetic fields from specific current distributions through direct solution of the Maxwell equations (Section 4.5) and through the intermediary of the vector potential (Section 4.6).

4.1 STATIC FIELD EQUATIONS WITH NO SOURCES

When there are no charges or currents present, the Maxwell equations have the form

$$\nabla \cdot \mathbf{E} = 0, \quad (4.1)$$

$$\nabla \times \mathbf{E} = 0, \quad (4.2)$$

$$\nabla \cdot \mathbf{B} = 0, \quad (4.3)$$

$$\nabla \times \mathbf{B} = 0. \quad (4.4)$$

These equations resolve into two decoupled and parallel sets for electric fields [Eqs. (4.1) and (4.2)] and magnetic fields [Eqs. (4.3) and (4.4)]. Equations (4.1)-(4.4) hold in regions such as that shown in Figure 4.1. The charges or currents that produce the fields are external to the volume of interest. In electrostatic calculations, the most common calculation involves charge distributed on the surfaces of conductors at the boundaries of a vacuum region.

Equations (4.1)-(4.4) have straightforward physical interpretations. Similar conclusions hold for both sets, so we will concentrate on electric fields. The form for the divergence equation [Eq. (4.1)] in Cartesian coordinates is

$$\partial E_x / \partial x + \partial E_y / \partial y + \partial E_z / \partial z = 0. \quad (4.5)$$

An example is illustrated in Figure 4.2. The electric field is a function of x and y . The meaning of the divergence equation can be demonstrated by calculating the integral of the normal electric field over the surface of a volume with cross-sectional area A and thickness Δx . The integral over the left-hand side is $AE_x(x)$. If the electric field is visualized in terms of vector field lines, the integral is the flux of lines into the volume through the left-hand face. The electric field line flux out of the volume through the right-hand face is $AE_x(x + \Delta x)$.

Steady State Electric and Magnetic Fields

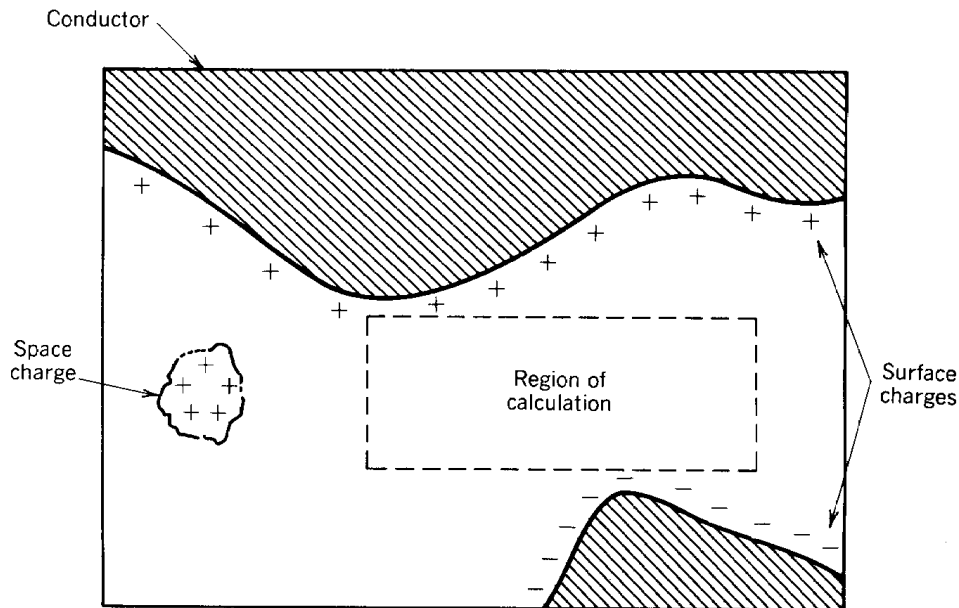


Figure 4.1 Calculation of static electric fields in a region with no source charge.

When the electric field is a smooth function of x , variations about a point can be approximated by a Taylor expansion. The right-hand integral is $A[E_x(x) + \Delta x \partial E_x / \partial x]$. The condition that $\partial E_x / \partial x = 0$ leads to a number of parallel conclusions.

1. The integrals of normal electric field over both faces of the volume are equal.
2. All field lines that enter the volume must exit.
3. The net flux of electric field lines into the volume is zero.
4. No field lines originate inside the volume.

Equation (4.5) is the three-dimensional equivalent of these statements.

The *divergence operator* applied to a vector quantity gives the effluence of the quantity away from a point in space. The divergence theorem can be written

$$\iint \mathbf{E} \cdot \mathbf{n} \, da = \iiint (\nabla \cdot \mathbf{E}) \, dV. \quad (4.6)$$

Equation (4.6) states that the integral of the divergence of a vector quantity over all points of a volume is equal to the surface integral of the normal component of the vector over the surface of the volume. With no enclosed charges, field lines must flow through a volume as shown in Figure 4.3. The same holds true for magnetic fields. The main difference between electric and magnetic fields is that magnetic field lines have zero divergence under all conditions, even in regions with currents. This means that magnetic field lines never emanate from a source point. They either extend indefinitely or are self-connected.

Steady State Electric and Magnetic Fields

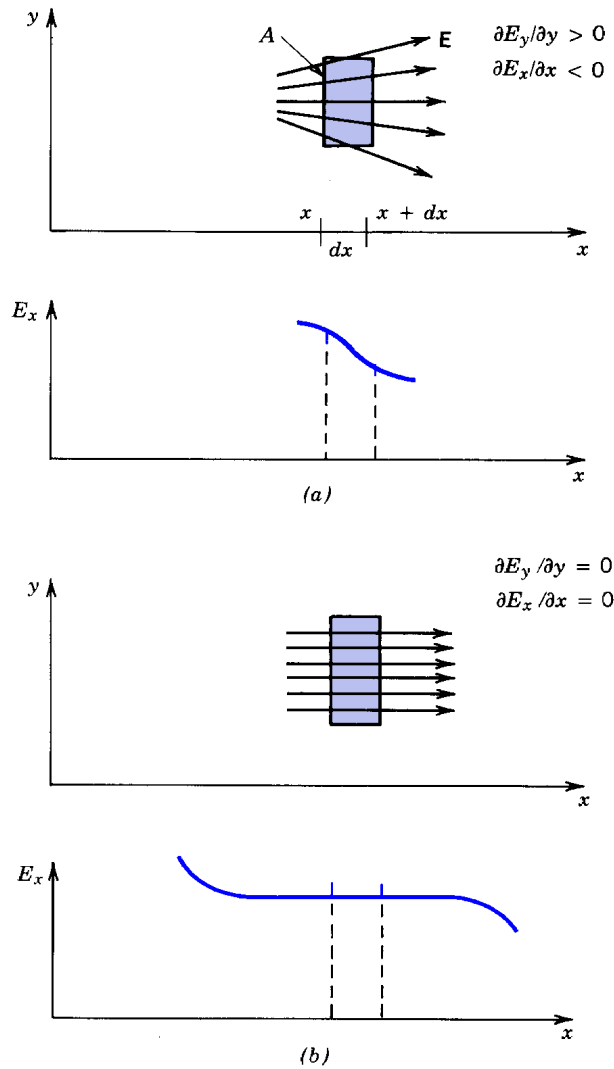


Figure 4.2 Relationship between gradients of electric field components and geometry of electric

The curl equations determine another geometric property of field lines. This property proceeds from the Stokes theorem, which states that

$$\int \mathbf{E} \cdot d\mathbf{l} = \iint (\nabla \times \mathbf{E}) \cdot \mathbf{n} \, da. \quad (4.7)$$

The quantities in Eq. (4.7) are defined in Figure 4.4; S is a two-dimensional surface in space and $d\mathbf{l}$ is a length element oriented along the circumference. The integral on the left-hand side is taken

Steady State Electric and Magnetic Fields

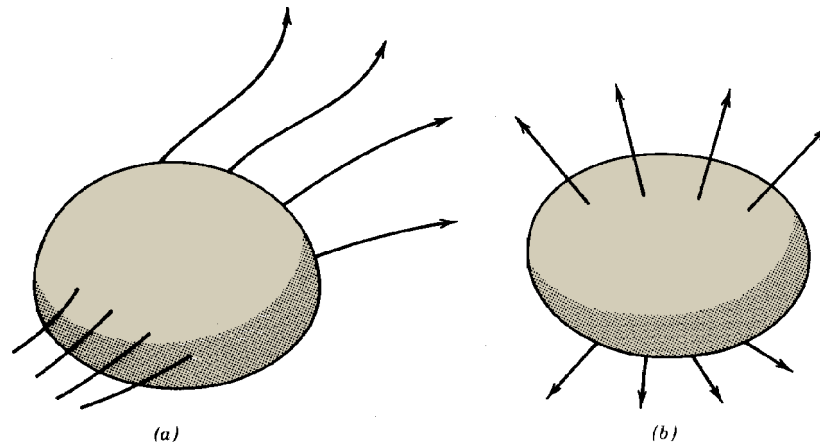


Figure 4.3 Geometry of vector field lines near a point with (a) zero divergence and (b) nonzero divergence.

around the periphery. The right-hand side is the surface integral of the component of the vector $\mathbf{v} \times \mathbf{E}$ normal to the surface. If the curl is nonzero at a point in space, then field lines form closed loops around the point. Figure 4.5 illustrates points in vector fields with zero and nonzero curl. The study of magnetic fields around current-carrying wires (Section 4.5) will illustrate a vector function with a nonzero curl.

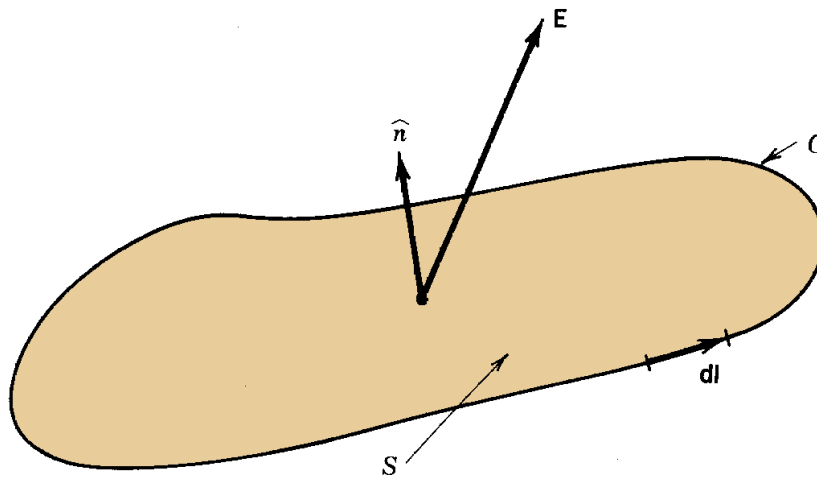


Figure 4.4 Definition of quantities used in Stokes theorem.

Steady State Electric and Magnetic Fields

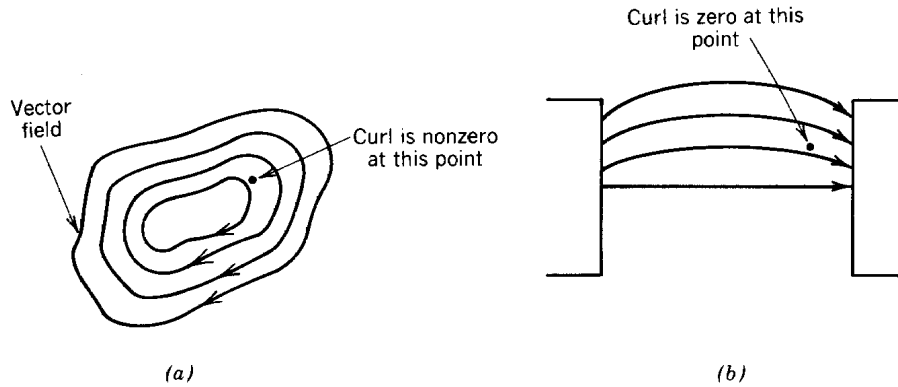


Figure 4.5 Geometry of vector field lines near a point with (a) nonzero curl and (b) zero curl.

For reference, the curl operator is written in Cartesian coordinates as

$$\nabla \times \mathbf{E} = \begin{bmatrix} \mathbf{u}_x & \mathbf{u}_y & \mathbf{u}_z \\ \partial/\partial x & \partial/\partial y & \partial/\partial z \\ E_x & E_y & E_z \end{bmatrix}. \quad (4.8)$$

The usual rule for evaluating a determinant is used. The expansion of the above expression is

$$\nabla \times = \mathbf{u}_x \left(\frac{\partial E_z}{\partial y} - \frac{\partial E_y}{\partial z} \right) + \mathbf{u}_y \left(\frac{\partial E_x}{\partial z} - \frac{\partial E_z}{\partial x} \right) + \mathbf{u}_z \left(\frac{\partial E_y}{\partial x} - \frac{\partial E_x}{\partial y} \right). \quad (4.9)$$

The electrostatic potential function ϕ can be defined when electric fields are static. The electric field is the gradient of this function,

$$\mathbf{E} = -\nabla\phi. \quad (4.10)$$

Substituting for \mathbf{E} in Eq. (4.1) gives

$$\nabla \cdot (\nabla\phi) = 0,$$

or

$$\nabla^2\phi = \partial^2\phi/\partial x^2 + \partial^2\phi/\partial y^2 + \partial^2\phi/\partial z^2 = 0. \quad (4.11)$$

The operator symbolized by ∇^2 in Eq. (4.11) is called the Laplacian operator. Equation (4.11) is the *Laplace equation*. It determines the variation of ϕ (and hence \mathbf{E}) in regions with no charge.

Steady State Electric and Magnetic Fields

The curl equation is automatically satisfied through the vector identity $\nabla \times (\nabla \phi) = 0$.

The main reason for using the Laplace equation rather than solving for electric fields directly is that boundary conditions can be satisfied more easily. The difficulty in solving the Maxwell equations directly lies in determining boundary conditions for vector fields on surrounding conducting surfaces. The electrostatic potential is a scalar function; we can show that the potential is a constant on a connected metal surface. Metals contain free electrons; an electric field parallel to the surface of a metal drives large currents. Electrons in the metal adjust their positions to produce a parallel component of field equal and opposite to the applied field. Thus, at a metal surface $\mathbf{E}(\text{parallel}) = 0$ and $\mathbf{E}(\text{normal})$ is unspecified. Equation (4.10) implies that electric field lines are always normal to surfaces of constant ϕ . This comes about because the gradient of a function (which indicates the direction in which a function has maximum rate of variation) must always be perpendicular to surfaces on which the function is constant (Fig. 4.6). Since a metal surface is everywhere perpendicular to the electric field, it must be an equipotential surface with the boundary condition $\phi = \text{constant}$.

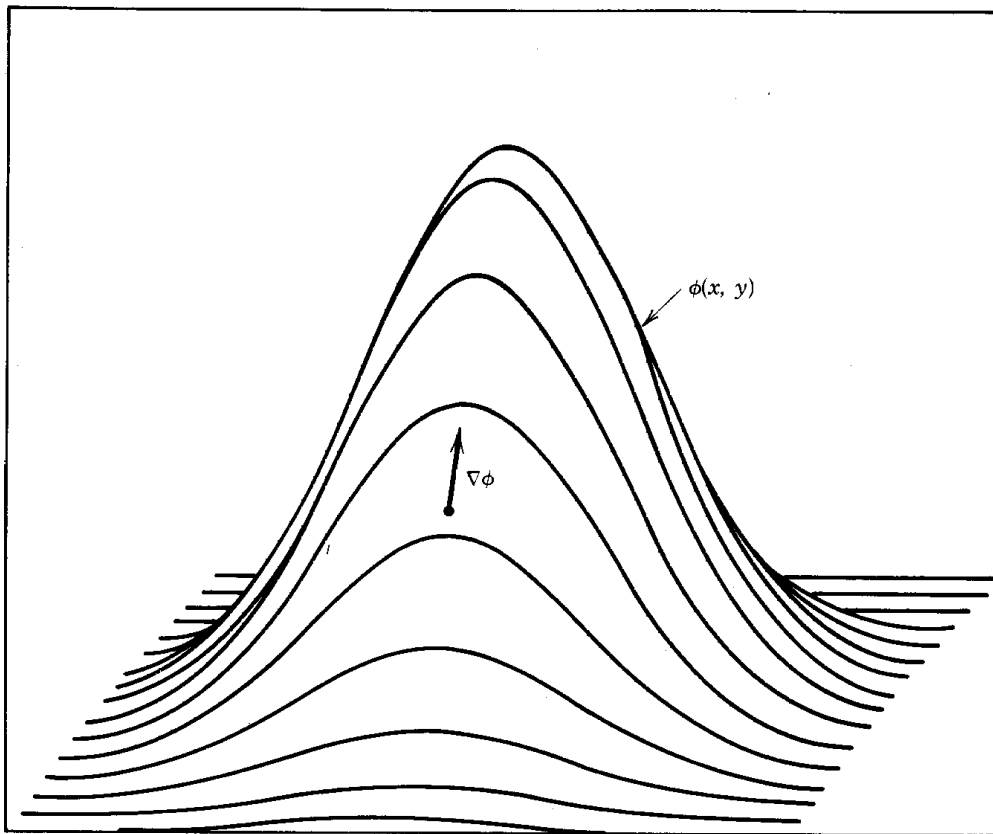


Figure 4.6 Three-dimensional plot of a scalar function $\phi(x, y)$, illustrating the orientation of the gradient vector $\nabla\phi$.

Steady State Electric and Magnetic Fields

In summary, electric field lines have the following properties in source-free regions:

- (a) Field lines are continuous. All lines that enter a volume eventually exit.
- (b) Field lines do not kink, curl, or cross themselves.
- (c) Field lines do not cross each other, since this would result in a point of infinite flux.
- (d) Field lines are normal to surfaces of constant electrostatic potential.
- (e) Electric fields are perpendicular to metal surfaces.

Fairly accurate electric field sketches can be made utilizing the laminar flow nature of electric field lines and the above properties. Even with the availability of digital computers, it is valuable to generate initial sketches of field patterns. This saves time and gives insight into the nature of fields. An example of an electrostatic field pattern generated by the method of squares is shown in

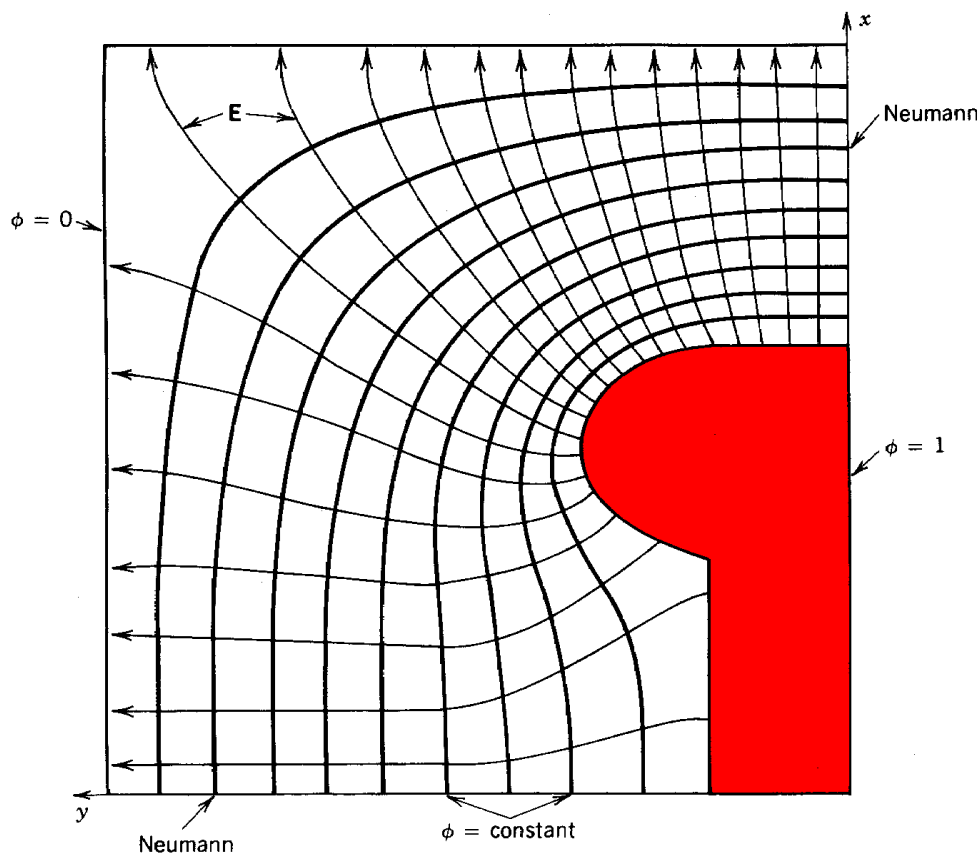


Figure 4.7 Equipotential lines and electric field lines around a high-voltage electrode in a grounded case. Electrode and case have infinite extent in z direction (out of page). Solution carried out only in one quadrant because of symmetry about x and y axes.

Steady State Electric and Magnetic Fields

Figure 4.7. In this method, a number of equipotential lines between metal surfaces are sketched. Electric field lines normal to the equipotential lines and electrodes are added. Since the density of field lines is proportional to the distance between equipotentials, a valid final solution results when the elements between equipotential and field lines approach as close as possible to squares. The process is iterative and requires only some drawing ability and an eraser.

It is also possible to define formally a magnetic potential U_m such that

$$\nabla^2 U_m = 0. \quad (4.12)$$

The function U_m should not be confused with the vector potential. Methods used for electric field problems in source-free regions can also be applied to determine magnetic fields. We will defer use of Eq. (4.12) to Chapter 5. An understanding of magnetic materials is necessary to determine boundary conditions for U_m .

4.2 NUMERICAL SOLUTIONS TO THE LAPLACE EQUATION

The Laplace equation determines electrostatic potential as a function of position. Resulting electric fields can then be used to calculate particle orbits. Electrostatic problems may involve complex geometries with surfaces at many different potentials. In this case, numerical methods of analysis are essential.

Digital computers handle discrete quantities, so the Laplace equation must be converted from a continuous differential equation to a finite difference formulation. As shown in Figure 4.8, the quantity $\Phi(i, j, k)$ is defined at discrete points in space. These points constitute a three-dimensional mesh. For simplicity, the mesh spacing Δ between points in the three Cartesian directions is assumed uniform. The quantity Φ has the property that it equals $\varphi(x, y, z)$ at the mesh points. If φ is a smoothly varying function, then a linear interpolation of Φ gives a good approximation for φ at any point in space. In summary, Φ is a mathematical construct used to estimate the physical quantity, φ .

The Laplace equation for φ implies an algebraic difference equation for Φ . The spatial position of a mesh point is denoted by (i, j, k) , with $x = i\Delta$, $y = j\Delta$, and $z = k\Delta$. The x derivative of φ to the right of the point (x, y, z) is approximated by

$$\partial\varphi(x+\Delta/2)/\partial x = [\Phi(i+1,j,k) - \Phi(i,j,k)]/\Delta. \quad (4.13)$$

A similar expression holds for the derivative at $x - \Delta/2$. The second derivative is the difference of derivatives divided by Δ , or

$$\frac{\partial}{\partial x} \left(\frac{\partial\varphi(x)}{\partial x} \right) \approx \frac{1}{\Delta} \left(\frac{\partial\varphi(x+\Delta/2)}{\partial x} - \frac{\partial\varphi(x-\Delta/2)}{\partial x} \right)$$

Steady State Electric and Magnetic Fields

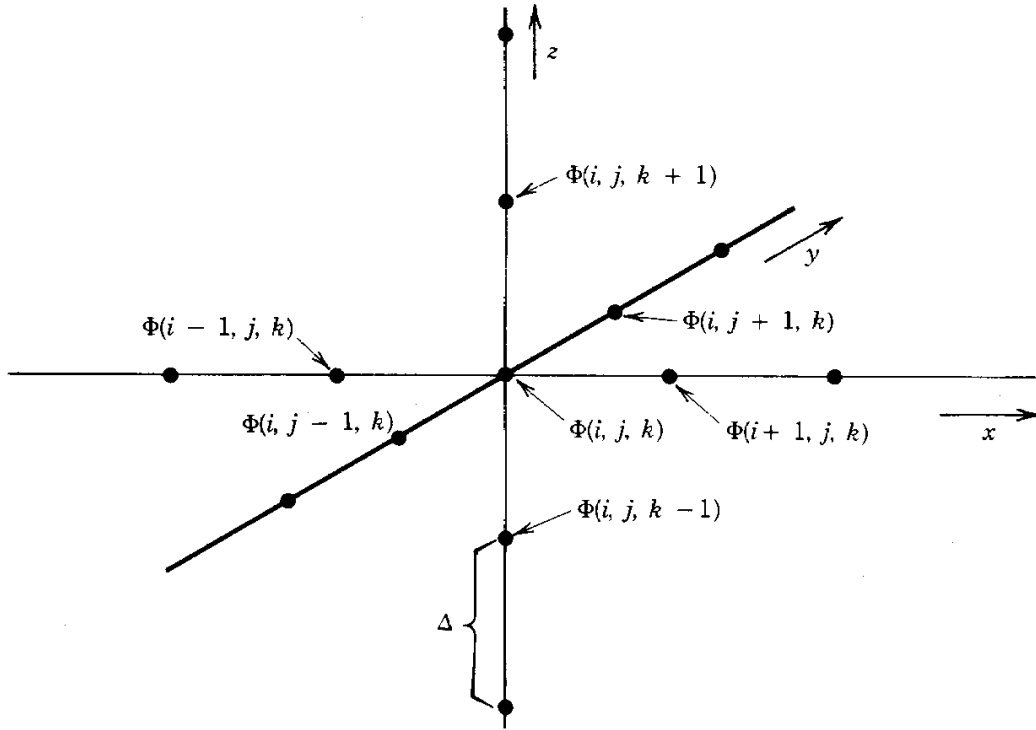


Figure 4.8 Finite difference approximation for electrostatic potential.

Combining expressions,

$$\frac{\partial^2 \Phi}{\partial x^2} = \frac{\Phi(i+1, j, k) - 2\Phi(i, j, k) + \Phi(i-1, j, k)}{\Delta^2} \quad (4.14)$$

Similar expressions can be found for the $\partial^2 \Phi / \partial y^2$ and $\partial^2 \Phi / \partial z^2$ terms. Setting $\nabla^2 \Phi = 0$ implies

$$\begin{aligned} \Phi(i, j, k) = & 1/6 [\Phi(i+1, j, k) + \Phi(i-1, j, k) + \Phi(i, j+1, k) \\ & + \Phi(i, j-1, k) + \Phi(i, j, k+1) + \Phi(i, j, k-1)]. \end{aligned} \quad (4.15)$$

In summary, (1) $\Phi(i, j, k)$ is a discrete function defined as mesh points, (2) the interpolation of $\Phi(i, j, k)$ approximates $\phi(x, y, z)$, and (3) if $\phi(x, y, z)$ satisfies the Laplace equation, then $\Phi(i, j, k)$ is determined by Eq. (4.15).

According to Eq. (4.15), individual values of $\Phi(i, j, k)$ are the average of their six neighboring

Steady State Electric and Magnetic Fields

points. Solving the Laplace equation is an averaging process; the solution gives the smoothest flow of field lines. The net length of all field lines is minimized consistent with the boundary conditions. Therefore, the solution represents the state with minimum field energy (Section 5.6).

There are many numerical methods to solve the finite difference form for the Laplace equation. We will concentrate on the *method of successive overrelaxation*. Although it is not the fastest method of solution, it has the closest relationship to the physical content of the Laplace equation. To illustrate the method, the problem will be formulated on a two-dimensional, square mesh. Successive overrelaxation is an iterative approach. A trial solution is corrected until it is close to a valid solution. Correction consists of sweeping through all values of an intermediate solution to calculate *residuals*, defined by

$$R(i,j) = \frac{1}{4}[\Phi(i+1,j) + \Phi(i-1,j) + \Phi(i,j+1) + \Phi(i,j-1)] - \Phi(i,j) \quad (4.16)$$

If $R(i, j)$ is zero at all points, then $\Phi(i, j)$ is the desired solution. An intermediate result can be improved by adding a correction factor proportional to $R(i, j)$,

$$\Phi(i,j)_{n+1} = \Phi(i,j)_n + \omega R(i,j)_n. \quad (4.17)$$

The value $\omega = 1$ is the obvious choice, but in practice values of ω between 1 and 2 produce a faster convergence (hence the term overrelaxation). The succession of approximations resembles a time-dependent solution for a system with damping, relaxing to its lowest energy state. The elastic sheet analog (described in Section 4.3) is a good example of this interpretation. Figure 4.9 shows intermediate solutions for a one-dimensional mesh with 20 points and with $\omega = 1.00$. Information on the boundary with elevated potential propagates through the mesh.

The method of successive overrelaxation is quite slow for large numbers of points. The number of calculations on an $n \times n$ mesh is proportional to n^2 . Furthermore, the number of iterations necessary to propagate errors out of the mesh is proportional to n . The calculation time increases as n^3 . A BASIC algorithm to relax internal points in a 40×48 point array is listed in Table 4.1. Corrections are made continuously during the sweep. Sweeps are first carried out along the x direction and then along the y direction to allow propagation of errors in both directions. The electrostatic field distribution in Figure 4.10 was calculated by a relaxation program.

Advanced methods for solving the Laplace equation generally use more efficient algorithms based on Fourier transforms. Most available codes to solve electrostatic problems utilize a more complex mesh. The mesh may have a rectangular or even triangular divisions to allow a close match to curved boundary surfaces.

Steady State Electric and Magnetic Fields

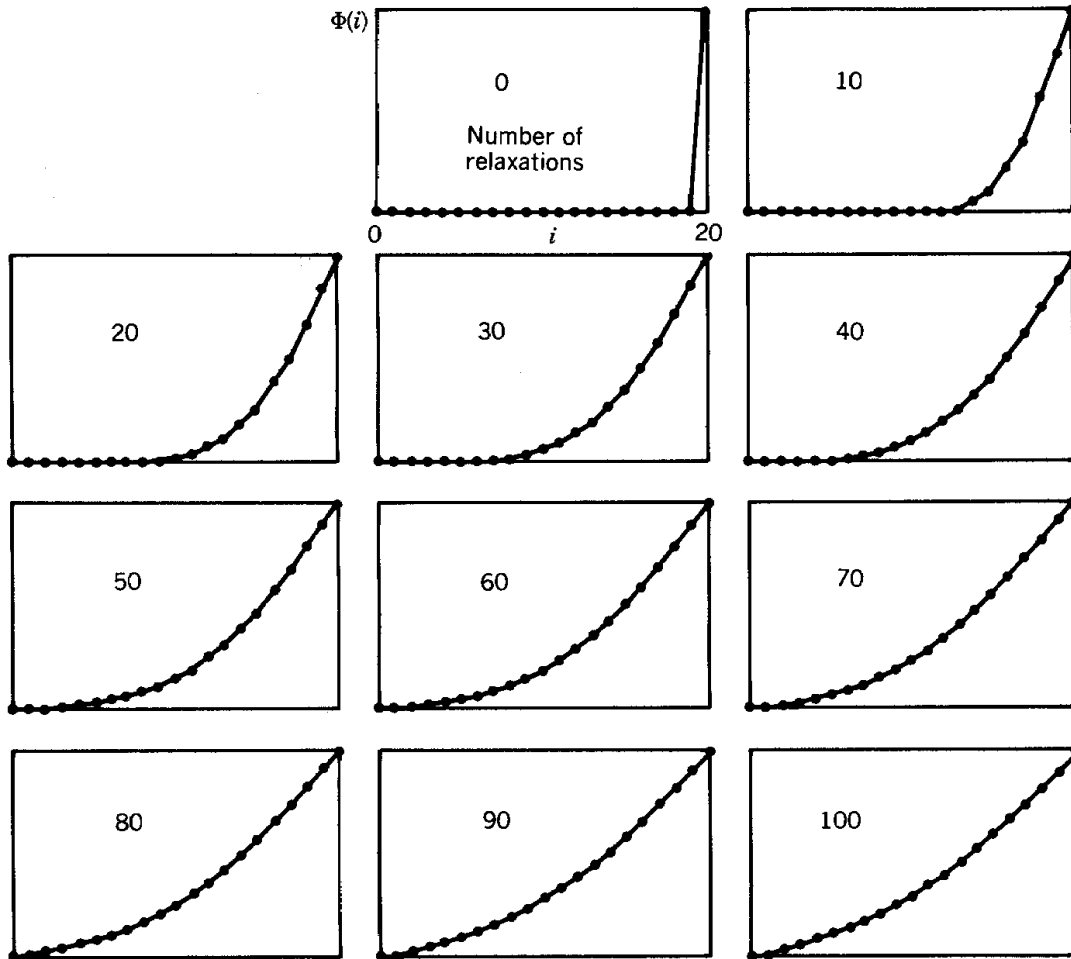


Figure 4.9 Relaxation method for solving the Laplace equation. Successive one-dimensional solutions for electrostatic potential between charged plates as a function of the number of mesh relaxations. Initial conditions: $\Phi(1) - \Phi(19) = 0$; $\Phi(20) = 1$.

Boundary conditions present special problems and must be handled differently from internal points representing the vacuum region. Boundary points may include those on the actual boundary of the calculational mesh, or points on internal electrodes maintained at a constant potential. The latter points are handled easily. They are marked by a flag to indicate locations of nonvariable potential. The relaxation calculation is not performed at such points. Locations on the mesh boundary have no neighbors outside the mesh, so that Eq. (4.16) can not be applied. If these points have constant potential, there is no problem since the residual need not be computed. Constant-potential points constitute a Dirichlet boundary condition.

The other commonly encountered boundary specification is the Neumann condition in which the normal derivative of the potential at the boundary is specified. In most cases where the Neumann condition is used, the derivative is zero, so that there is no component of the electric field normal

Steady State Electric and Magnetic Fields

TABLE 4.1 Subroutines: Successive Over-Relaxation Program

```

1000 REM --- RELAXATION SUBROUTINES FOR POINTS
1010 REM --- INTERNAL TO BOUNDARY

1200 REM --- SWEEP ALONG I DIRECTION
1202 FOR J=1 TO JMAX
1204 FOR I=1 TO IMAX
1206 IF IB(I,J)<>0 THEN GOTO 1212:REM --- SPECIFIED POTENTIAL
1208 RES = (P(I+1,J)+P(I-1,J)+P(I,J+1)+P(I,J-1)) / 4 - P(I,J)
1210 P(I,J) = P(I,J) + OMEGA*RES
1212 NEXT I
1214 NEXT J
1216 RETURN

1300 REM --- SWEEP ALONG J DIRECTION
1302 FOR I=1 TO IMAX
1304 FOR J=1 TO JMAX
1306 IF IB(I,J)<>0 THEN GOTO 1312:REM --- SPECIFIED POTENTIAL
1308 RES = (P(I+1,J)+P(I-1,J)+P(I,J+1)+P(I,J-1)) / 4 - P(I,J)
1310 P(I,J) = P(I,J) + OMEGA*RES
1312 NEXT J
1314 NEXT I
1316 RETURN

```

to the boundary. This condition applies to boundaries with special symmetry, such as the axis in a cylindrical calculation or a symmetry plane of a periodic system. Residues can be calculated at Neumann boundaries since the potential outside the mesh is equal to the potential at the first point inside the mesh. For example, on the boundary $i = 0$, the condition $\Phi(-1, j) = \Phi(+1, j)$ holds. The residual is

$$R(0,j) = \frac{1}{4} [\Phi(0,j+1) + 2\Phi(1,j) + \Phi(0,j-1)] - \Phi(0,j). \quad (4.18)$$

Two-dimensional systems with cylindrical symmetry are often encountered in accelerator applications. Potential is a function of (r, z) , with no azimuthal dependence. The Laplace equation for a cylindrical system is

$$\frac{1}{r} \frac{\partial}{\partial r} \left(r \frac{\partial \phi}{\partial r} \right) + \frac{\partial^2 \phi}{\partial z^2} = 0. \quad (4.19)$$

The finite difference form for the Laplace equation for this case is

Steady State Electric and Magnetic Fields

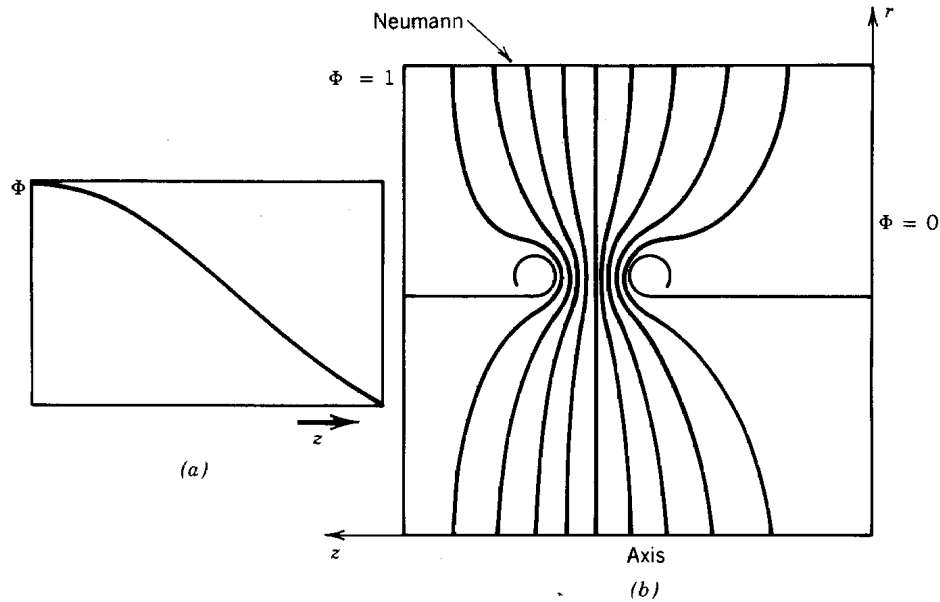


Figure 4.10 Two-dimensional solution for equipotentials between cylindrical electrodes of a drift tube linear accelerator calculated by the method of successive overrelaxation ($\omega = 1.75$). (a) Variation of potential on axis, $\Phi(0, z)$. (b) Boundary conditions, equipotential lines.

$$\Phi(i, j) = \frac{1}{4} \left[\frac{(i+1/2)\Phi(i+1, j)}{i} + \frac{(i-1/2)\Phi(i-1, j)}{i} + \Phi(i, j+1) + \Phi(i, j-1) \right]. \quad (4.20)$$

where $r = i\Delta$ and $z = j\Delta$.

Figure 4.10 shows results for a relaxation calculation of an electrostatic immersion lens. It consists of two cylinders at different potentials separated by a gap. Points of constant potential and Neumann boundary conditions are indicated. Also shown is the finite difference approximation for the potential variation along the axis, $\Phi(0, z)$. This data can be used to determine the focal properties of the lens (Chapter 6).

4.3 ANALOG METHODS TO SOLVE THE LAPLACE EQUATION

Analog methods were used extensively to solve electrostatic field problems before the advent of digital computers. We will consider two analog techniques that clarify the nature of the Laplace equation. The approach relies on finding a physical system that obeys the Laplace equation but that allows easy measurements of a characteristic quantity (the analog of the potential).

One system, the tensioned elastic sheet, is suitable for two-dimensional problems (symmetry

Steady State Electric and Magnetic Fields

along the z axis). As shown in Figure 4.11, a latex sheet is stretched with uniform tension on a frame. If the sheet is displaced vertically a distance $H(x, y)$, there will be vertical restoring forces. In equilibrium, there is vertical force balance at each point. The equation of force balance can be determined from the finite difference approximation defined in Figure 4.11. In terms of the surface tension, the forces to the left and right of the point $(i\Delta, j\Delta)$ are

$$F[(i-1/2)\Delta] = T [H(i\Delta, j\Delta) - H([i-1]\Delta, j\Delta)]/\Delta,$$

$$F[(i+1/2)\Delta] = T [H([i+1]\Delta, j\Delta) - H(i\Delta, j\Delta)]/\Delta.$$

Similar expressions can be determined for the y direction. The height of the point $(i\Delta, j\Delta)$ is constant in time; therefore,

$$F[(i-1/2)\Delta] = -F[(i+1/2)\Delta],$$

and

$$F[(j+1/2)\Delta] = -F[(j-1/2)\Delta].$$

Substituting for the forces shows that the height of a point on a square mesh is the average of its four nearest neighbors. Thus, inverting the arguments of Section 4.2, $H(x, y)$ is described by the two-dimensional Laplace equation

$$\partial^2 H(x, y) / \partial x^2 + \partial^2 H(x, y) / \partial y^2 = 0.$$

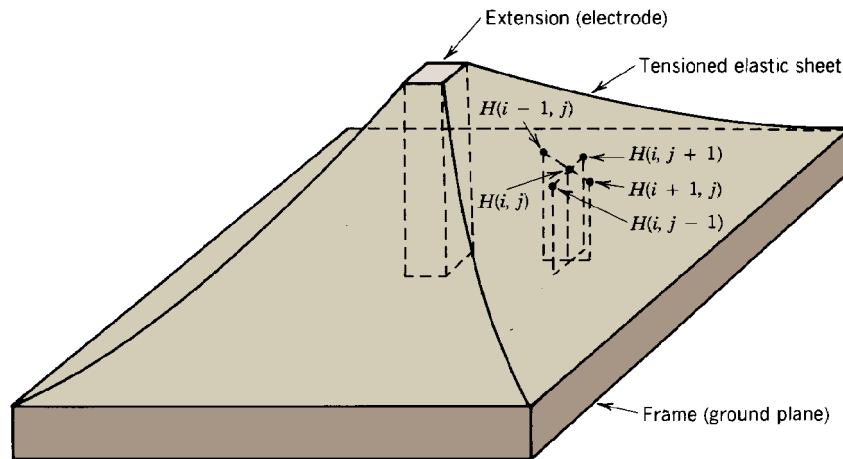


Figure 4.11 Tensioned elastic sheet analog for electrostatic potential.

Steady State Electric and Magnetic Fields

Height is the analog of potential. To make an elastic potential solution, parts are cut to the shape of the electrodes. They are fastened to the frame to displace the elastic sheet up or down a distance proportional to the electrode potential. These pieces determine equipotential surfaces. The frame is the ground plane.

An interesting feature of the elastic sheet analog is that it can also be used to determine orbits of charged particles in applied electrostatic fields. Neglecting rotation, the total energy of a ball bearing on the elastic sheet is $E = T + mgh(x, y)$, where g is the gravitational constant. The transverse forces acting on a ball bearing on the elastic sheet are $F_x = \partial H / \partial x$ and $F_y = \partial H / \partial y$. Thus, ball bearings on the elastic sheet follow the same orbits as charged particles in the analogous electrostatic potential, although over a considerably longer time scale.

Figure 4.12 is a photograph of a model that demonstrates the potentials in a planar electron extraction gap with a coarse grid anode made of parallel wires. The source of the facet lens effect associated with extraction grids (Section 6.5) is apparent.

A second analog technique, the electrolytic tank, permits accurate measurements of potential distributions. The method is based on the flow of current in a liquid medium of constant-volume resistivity, ρ (measured in units of ohm-meters). A dilute solution of copper sulfate in water is a common medium. A model of the electrode structure is constructed to scale from copper sheet and immersed in the solution. Alternating current voltages with magnitude proportional to those in the actual system are applied to the electrodes.

According to the definition of volume resistivity, the current density is proportional to the electric field

$$\mathbf{E} = \rho \mathbf{j}$$

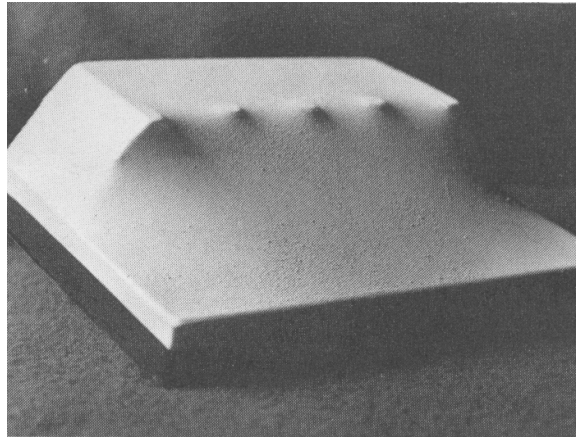


Figure 4.12 Elastic sheet analog for electrostatic potential near an extraction grid. Elevated section represents a high-voltage electrode surrounded by a grounded enclosure. Note the distortion of the potential near the grid wires that results in focusing of extracted particles. (Photograph and model by the author. Latex courtesy of the Hygenic Corporation.)

Steady State Electric and Magnetic Fields

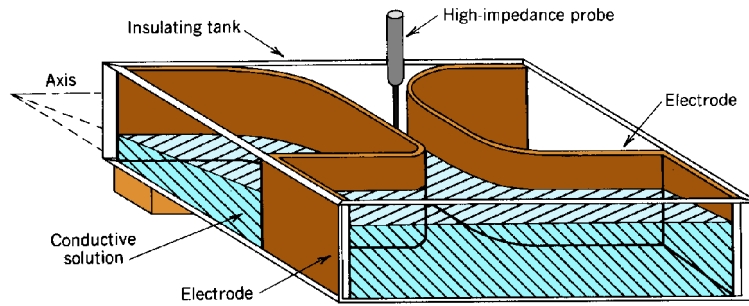


Figure 4.13 Electrolytic tank analog to solve the Laplace equation in a cylindrically symmetric system.

or

$$\mathbf{j} = -\nabla\phi/\rho. \quad (4.21)$$

The steady-state condition that charge at any point in the liquid is a constant implies that all current that flows into a volume element must flow out. This condition can be written

$$\nabla \cdot \mathbf{j} = 0. \quad (4.22)$$

Combining Eq. (4.21) with (4.22), we find that potential in the electrolytic solution obeys the Laplace equation.

In contrast to the potential in the real system, the potential in the electrolytic analog is maintained by a real current flow. Thus, energy is available for electrical measurements. A high-impedance probe can be inserted into the solution without seriously perturbing the fields. Although the electrolytic method could be applied to three-dimensional problems, in practice it is usually limited to two-dimensional simulations because of limitations on insertion of a probe. A typical setup is shown in Figure 4.13. Following the arguments given above, it is easy to show that a tipped tank can be used to solve for potentials in cylindrically symmetric systems.

4.4 ELECTROSTATIC QUADRUPOLE FIELD

Although numerical calculations are often necessary to determine electric and magnetic fields in accelerators, analytic calculations have advantages when they are tractable. Analytic solutions show general features and scaling relationships. The field expressions can be substituted into equations of motion to yield particle orbit expressions in closed form. Electrostatic solutions for a wide variety of electrode geometries have been derived. In this section, we will examine the quadrupole field, a field configuration used in all high-energy transport systems. We will concentrate on the electrostatic quadrupole; the magnetic equivalent will be discussed in Chapter

Steady State Electric and Magnetic Fields

5.

The most effective procedure to determine electrodes to generate quadrupole fields is to work in reverse, starting with the desired electric field distribution and calculating the associated potential function. The equipotential lines determine a set of electrode surfaces and potentials that generate the field. We assume the following two-dimensional fields:

$$E_x = +kx = E_o x/a, \quad (4.23)$$

$$E_y = -ky = -E_o y/a. \quad (4.24)$$

It is straightforward to verify that both the divergence and curl of \mathbf{E} are zero. The fields of Eqs. (4.23) and (4.24) represent a valid solution to the Maxwell equations in a vacuum region. The electric fields are zero at the axis and increase (or decrease) linearly with distance from the axis. The potential is related to the electric field by

$$\partial\phi/\partial x = -E_o x/a, \quad \partial\phi/\partial y = +E_o y/a,$$

Integrating the partial differential equations

$$\phi = -E_o x^2/2a + f(y) + C, \quad \phi = +E_o y^2/2a + g(x) + C'.$$

Taking $\phi(0, 0) = 0$, both expressions are satisfied if

$$\phi(x,y) = (E_o/2a) (y^2 - x^2). \quad (4.25)$$

This can be rewritten in a more convenient, dimensionless form:

$$\frac{\phi(x,y)}{E_o a/2} = \left(\frac{y}{a}\right)^2 - \left(\frac{x}{a}\right)^2. \quad (4.26)$$

Equipotential surfaces are hyperbolas in all four quadrants. There is an infinite set of electrodes that will generate the fields of Eqs. (4.23) and (4.24). The usual choice is symmetric electrodes on the equipotential lines $\phi_o = \pm E_o a/2$. Electrodes, field lines, and equipotential surfaces are plotted in Figure 4.14. The quantity a is the minimum distance from the axis to the electrode, and E_o is the electric field on the electrode surface at the position closest to the origin. The equipotentials in Figure 4.14 extend to infinity. In practice, focusing fields are needed only near the axis. These fields are not greatly affected by terminating the electrodes at distances a few times a from the axis.

Steady State Electric and Magnetic Fields

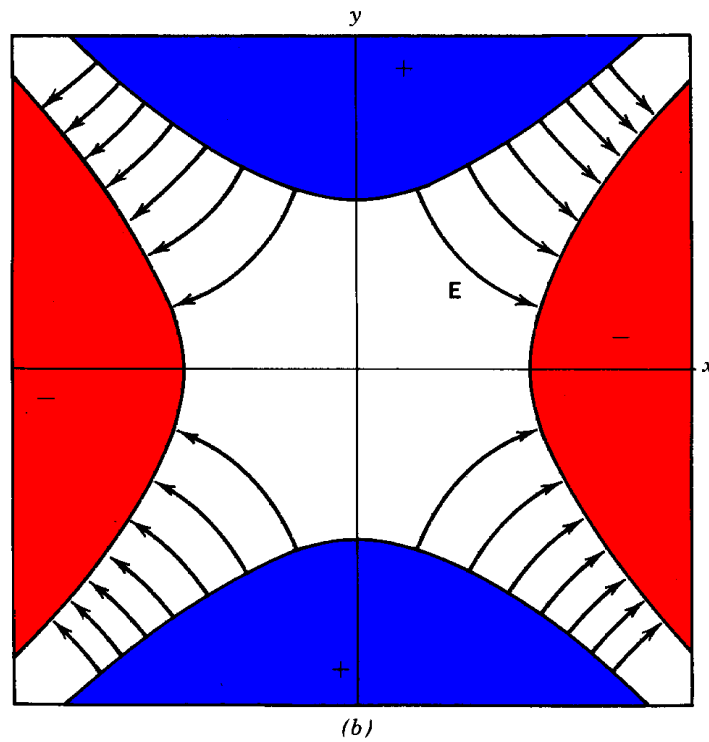
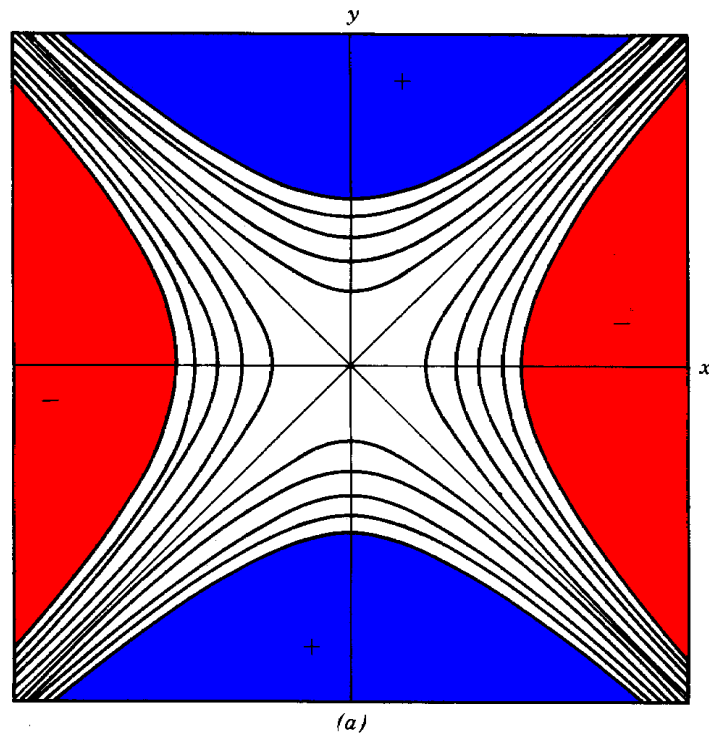


Figure 4.14 Electrostatic quadrupole field. (a) Equipotential lines. (b) Field lines.

4.5 STATIC ELECTRIC FIELDS WITH SPACE CHARGE

Space charge is charge density present in the region in which an electric field is to be calculated. Clearly, space charge is not included in the Laplace equation, which describes potential arising from charges on external electrodes. In accelerator applications, space charge is identified with the charge of the beam; it must be included in calculations of fields internal to the beam. Although we will not deal with beam self-fields in this book, it is useful to perform at least one space charge calculation. It gives insight into the organization of various types of charge to derive electrostatic solutions. Furthermore, we will derive a useful formula to estimate when beam charge can be neglected.

Charge density can be conveniently divided into three groups: (1) applied, (2) dielectric, and (3) space charge. Equation 3.13 can be rewritten

$$\nabla \cdot \mathbf{E} = (\rho_1 + \rho_2 + \rho_3)/\epsilon_0. \quad (4.27)$$

The quantity ρ_1 is the charge induced on the surfaces of conducting electrodes by the application of voltages. The second charge density represents charges in *dielectric materials*. Electrons in dielectric materials cannot move freely. They are bound to a positive charge and can be displaced only a small distance. The dielectric charge density can influence fields in and near the material. Electrostatic calculations with the inclusion of ρ_2 are discussed in Chapter 5. The final charge density, ρ_3 , represents space charge, or free charge in the region of the calculation. This usually includes the charge density of the beam. Other particles may contribute to ρ_3 , such as low-energy electrons in a neutralized ion beam.

Electric fields have the property of superposition. Given fields corresponding to two or more charge distributions, then the total electric field is the vector sum of the individual fields if the charge distributions do not perturb one another. For instance, we could calculate electric fields individually for each of the charge components, \mathbf{E}_1 , \mathbf{E}_2 , and \mathbf{E}_3 . The total field is

$$\mathbf{E} = \mathbf{E}_1(\text{applied}) + \mathbf{E}_2(\text{dielectric}) + \mathbf{E}_3(\text{spacecharge}). \quad (4.28)$$

Only the third component occurs in the example of Figure 4.15. The cylinder with uniform charge density is a commonly encountered approximation for beam space charge. The charge density is constant, ρ_0 , from $r = 0$ to $r = r_0$. There is no variation in the axial (z) or azimuthal (θ) directions so that $\partial/\partial z = \partial/\partial \theta = 0$. The divergence equation (3.13) implies that there is only a radial component of electric field. Because all field lines radiate straight outward (or inward for $\rho_0 < 0$), there can be no curl, and Eq. (3.11) is automatically satisfied.

Steady State Electric and Magnetic Fields

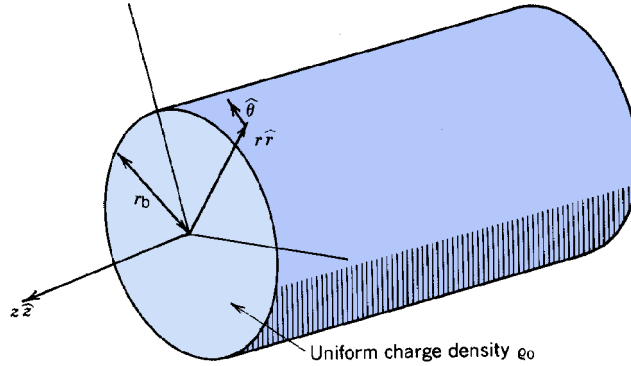


Figure 4.15 Quantities for calculating electric fields in and around a cylinder with uniform charge density (ρ_0).

Inside the charge cylinder, the electric field is determined by

$$\frac{1}{r} \frac{d(rE_r)}{dr} = \frac{\rho_o}{\epsilon_o} . \quad (4.29)$$

Electric field lines are generated by the charge inside a volume. The size of the radial volume element goes to zero near the origin. Since no field lines can emerge from the axis, the condition $E_r(r = 0) = 0$ must hold. The solution of Eq. (4.29) is

$$E_r(r < r_b) = \frac{\rho_o r}{2\epsilon_o} . \quad (4.30)$$

Outside the cylinder, the field is the solution of Eq. (4.29) with the right-hand side equal to zero. The electric field must be a continuous function of radius in the absence of a charge layer. (A charge layer is a finite quantity of charge in a layer of zero thickness; this is approximately the condition on the surface of an electrode.) Thus, $E_r(r = r_b^+) = E_r(r = r_b^-)$, so that

$$E_r(r > r_b) = \frac{\rho_o r_b^2}{2\epsilon_o r} . \quad (4.31)$$

The solution is plotted in Figure 4.16. The electric field increases linearly away from the axis in the charge region. It decreases as $1/r$ for $r > r_b$ because the field lines are distributed over a larger area.

The problem of the charge cylinder can also be solved through the electrostatic potential. The Poisson equation results when the gradient of the potential is substituted in Eq. (3.13):

Steady State Electric and Magnetic Fields

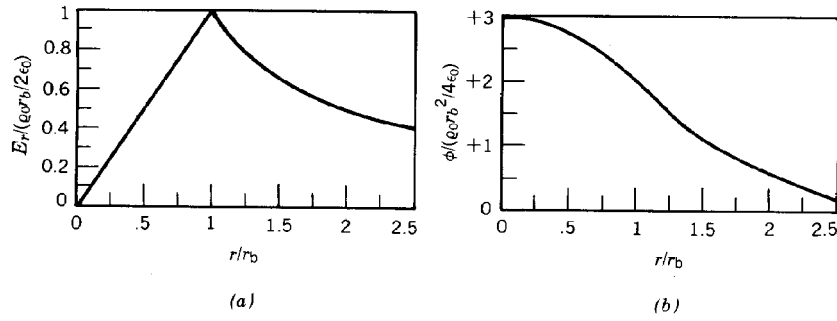


Figure 4.16 Solutions for the electrostatic fields of a cylinder with uniform charge density. (a) Normalized radial electric field $E_r / (\rho_0 r_b / 2 \epsilon_0)$. (b) Normalized electrostatic potential, $\phi / (\rho_0 r_b^2 / 4 \epsilon_0)$.

$$\nabla^2 \phi = -\frac{\rho(x)}{\epsilon_0}, \quad (4.32)$$

or

$$\frac{1}{r} \frac{d}{dr} \left(r \frac{d\phi}{dr} \right) = -\frac{\rho_o}{\epsilon_o}. \quad (4.33)$$

The solution to the Poisson equation for the charge cylinder is

$$\phi(r < r_b) = -\frac{\rho_o r^2}{4\epsilon_o}, \quad (4.34)$$

$$\phi(r > r_b) = -\frac{\rho_o r_b^2}{4\epsilon_o} \left(2 \ln \frac{r}{r_b} + 1 \right). \quad (4.35)$$

The potential is also plotted in Figure 4.16.

The Poisson equation can be solved by numerical methods developed in Section 4.2. If the finite difference approximation to $\nabla^2 \phi$ [Eq. (4.14)] is substituted in the Poisson equation in Cartesian coordinates (4.32) and both sides are multiplied by Δ^2 , the following equation results:

$$\begin{aligned} & -6\Phi(i,j,k) + \Phi(i+1,j,k) + \Phi(i-1,j,k) + \Phi(i,j+1,k) \\ & + \Phi(i,j-1,k) + \Phi(i,j,k+1) + \Phi(i,j,k-1) = -\rho(x,y,z)\Delta^3/\Delta\epsilon_o. \end{aligned} \quad (4.36)$$

Steady State Electric and Magnetic Fields

The factor $\rho\Delta^3$ is approximately the total charge in a volume Δ^3 surrounding the mesh point (i, j, k) when (1) the charge density is a smooth function of position and (2) the distance Δ is small compared to the scale length for variations in ρ . Equation (4.36) can be converted to a finite difference equation by defining $Q(i, j, k) = \rho(x, y, z)\Delta^3$. Equation (4.36) becomes

$$\begin{aligned} \Phi(i,j,k) = 1/6 [\Phi(i+1,j,k) + \Phi(i-1,j,k) + \Phi(i,j+1,k) \\ + \Phi(i,j-1,k) + \Phi(i,j,k+1) + \Phi(i,j,k-1)] + Q(i,j,k)/6\epsilon_o. \end{aligned} \quad (4.37)$$

Equation (4.37) states that the potential at a point is the average of its nearest neighbors elevated (or lowered) by a term proportional to the space charge surrounding the point.

The method of successive relaxation can easily be modified to treat problems with space charge. In this case, the residual [Eq. (4.16)] for a two-dimensional problem is

$$\begin{aligned} R(i,j) = 1/4 [\Phi(i+1,j) + \Phi(i-1,j) + \Phi(i,j+1) + \Phi(i,j-1)] \\ - \Phi(i,j) + Q(i,j)/4\epsilon_o. \end{aligned} \quad (4.38)$$

4.6 MAGNETIC FIELDS IN SIMPLE GEOMETRIES

This section illustrates some methods to find static magnetic fields by direct use of the Maxwell equations [(4.3) and (4.4)]. The fields are produced by current-carrying wires. Two simple, but often encountered, geometries are included: the field outside a long straight wire and the field inside of solenoidal winding of infinite extent.

The wire (Fig. 4.17) has current I in the z direction. There are no radial magnetic field lines since $\nabla \cdot \mathbf{B} = 0$. There is no component B_z since the fields must be perpendicular to the current. Thus, magnetic field lines are azimuthal. By symmetry, the field lines are circles. The magnitude of the azimuthal field (or density of lines) can be determined by rewriting the static form of Eq. (3.12) in integral form according to the Stokes law [Eq. (4.7)],

$$\int \mathbf{B} \cdot d\mathbf{l} = \mu_o \iint j_z dA = \mu_o I. \quad (4.39)$$

Using the fact that field lines are circles, we find that

$$B_\theta = \mu_o I / 2\pi r. \quad (4.40)$$

Steady State Electric and Magnetic Fields

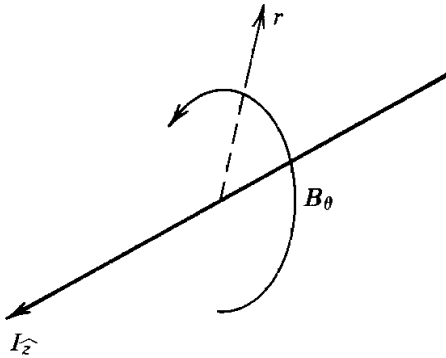


Figure 4.17 Magnetic field lines near a current-carrying wire.

The solenoidal coil is illustrated in Figure 4.18. It consists of a helical winding of insulated wire on a cylindrical mandrel. The wire carries current I . The quantity (N/L) is the number of turns per unit length. *Solenoid* derives from the Greek word for pipe; magnetic field lines are channeled through the windings. In a finite length winding, the field lines return around the outside. We will consider the case of an infinitely long structure with no axial variations. Furthermore, we assume there are many windings over a length comparable to the coil radius, or $(N/L)r_c \gg 1$. In this limit, we can replace the individual windings with a uniform azimuthal current sheet. The sheet has a current per unit length J (A/m) $= (N/L)I$.

The current that produces the field is azimuthal. By the law of Biot and Savart, there can be no component of azimuthal magnetic field. By symmetry, there can be no axial variation of field. The conditions of zero divergence and curl of the magnetic field inside the winding are written

$$\frac{1}{r} \frac{\partial(rB_r)}{\partial r} + \frac{\partial B_z}{\partial z} = 0, \quad \frac{\partial B_r}{\partial z} - \frac{\partial B_z}{\partial r} = 0. \quad (4.41)$$

Setting $\partial/\partial z$ equal to zero in Eqs. (4.41); we find that B_r is zero and that B_z has equal magnitude at all radii. The magnitude of the axial field can be determined by applying Eq. (4.39) to the loop illustrated in Figure 4.18. The field outside a long solenoid is negligible since return magnetic flux is spread over a large area. There are no contributions to the loop integral from the radial segments because fields are axial. The only component of the integral comes from the part of the path inside the solenoid, so that

$$B_o = \mu_o J = \mu_o (N/L) I. \quad (4.42)$$

Many magnetic confinement systems for intense electron beams or for high-temperature plasmas are based on a solenoidal coil bent in a circle and connected, as shown in Figure 4.19. The geometry is that of a doughnut or *torus* with circular cross section. The axial fields that circulate

Steady State Electric and Magnetic Fields

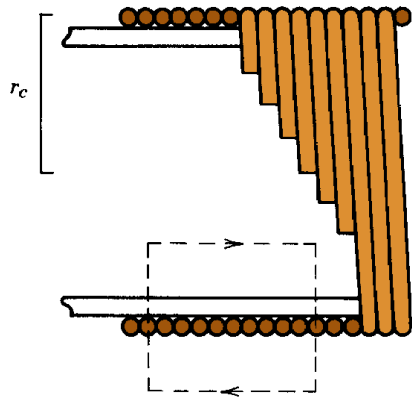


Figure 4.18 Solenoidal magnet coil.

around the torus are called *toroidal field lines*. Field lines are continuous and self-connected. All field lines are contained within the winding. The toroidal field magnitude inside the winding is not uniform. Modification of the loop construction of Figure 4.19 shows that the field varies as the inverse of the major radius. Toroidal field variation is small when the minor radius (the radius of the solenoidal windings) is much less than the major radius.

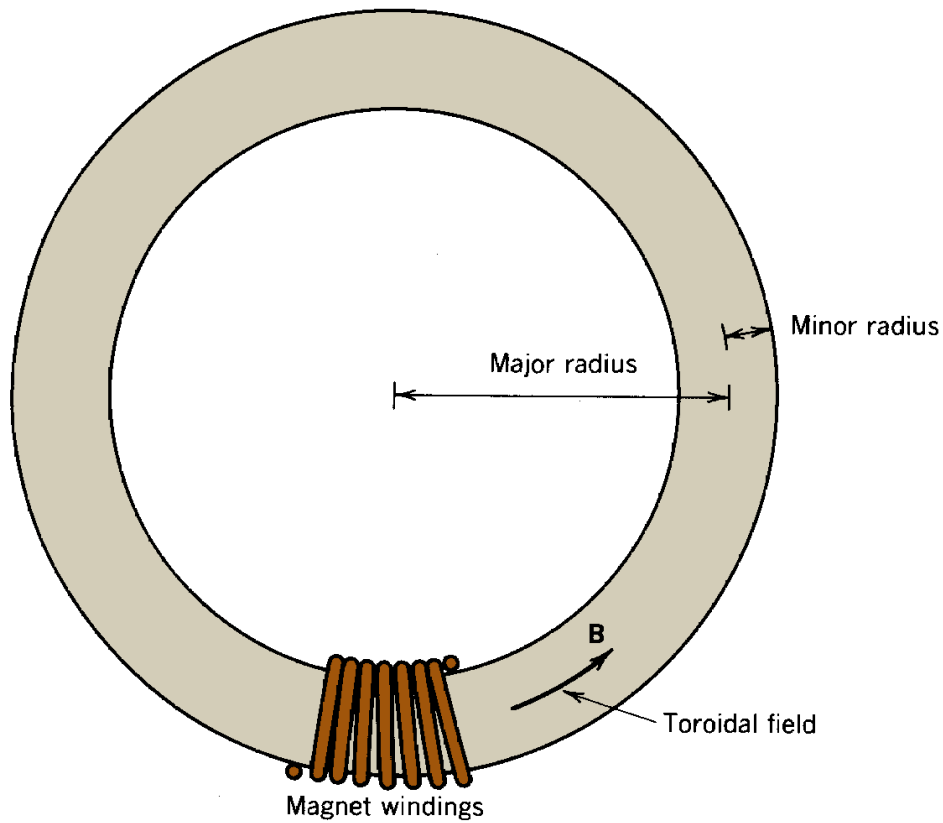


Figure 4.19 Toroidal magnet coil.

Steady State Electric and Magnetic Fields

4.7 MAGNETIC POTENTIALS

The magnetic potential and the vector potential aid in the calculation of magnetic fields. In this section, we will consider how these functions are related and investigate the physical meaning of the vector potential in a two-dimensional geometry. The vector potential will be used to derive the magnetic field for a circular current loop. Assemblies of loop currents are used to generate magnetic fields in many particle beam transport devices.

In certain geometries, magnetic field lines and the vector potential are closely related. Figure 4.20 illustrates lines of constant vector potential in an axially uniform system in which fields are generated by currents in the z direction. Equation (3.24) implies that the vector potential has only an axial component, A_z . Equation (3.23) implies that

$$B_x = \partial A_z / \partial y, \quad B_y = -\partial A_z / \partial x. \quad (4.43)$$

Figure 4.20 shows a surface of constant A_z in the geometry considered. This line is defined by

$$dA_z = 0 = (\partial A_z / \partial x) dx + (\partial A_z / \partial y) dy. \quad (4.44)$$

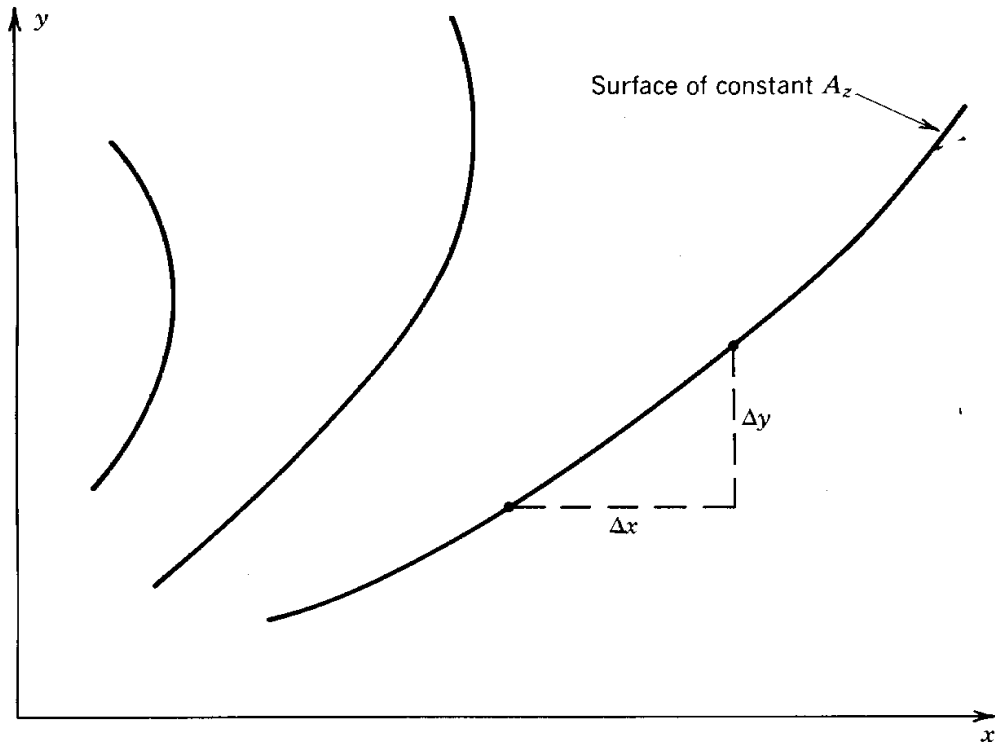


Figure 4.20 Lines of constant vector potential A_z . Two-dimensional system, symmetric along the z direction (out of page), axial currents only (j_z).

Steady State Electric and Magnetic Fields

Substituting Eqs. (4.43) into Eq. (4.44), an alternate equation for a constant A_z line is

$$dy/dx = B_y/B_x. \quad (4.45)$$

Equation (4.45) is also the equation for a magnetic field line. To summarize, when magnetic fields are generated by axial currents uniform in z , magnetic field lines are defined by lines of constant A_z .

A similar construction shows that magnetic field lines are normal to surfaces of constant magnetic potential. In the geometry of Figure 4.20,

$$B_x = \partial U_m / \partial x, \quad B_y = \partial U_m / \partial y. \quad (4.46)$$

by the definition of U_m . The equation for a line of constant U_m is

$$dU_m = (\partial U_m / \partial x) dx + (\partial U_m / \partial y) dy = B_x dx + B_y dy.$$

Lines of constant magnetic potential are described by the equation

$$dy/dx = -B_y/B_x. \quad (4.47)$$

Analytic geometry shows that the line described by Eq. (4.47) is perpendicular to that of Eq. (4.45).

The correspondence of field lines and lines of constant A_z can be used to find magnetic fields of arrays of currents. As an example, consider the geometry illustrated in Figure 4.21. Two infinite length wires carrying opposed currents $\pm I$ are separated by a distance $2d$. It is not difficult to show that the vector potential for a single wire is

$$A_z = \pm \frac{1}{2} \mu_o I \ln(x'^2 + y'^2) / 2\pi.$$

where the origin of the coordinate system (x', y') is centered on the wire. The total vector potential is the sum of contributions from both wires. In terms of the coordinate system (x, y) defined in Figure 4.21, the total vector potential is

$$A_z = \frac{\mu_o I}{4\pi} \ln \left(\frac{(x-d)^2 + y^2}{(x+d)^2 + y^2} \right).$$

Lines of constant A_z (corresponding to magnetic field lines) are plotted in Figure 4.21.

Steady State Electric and Magnetic Fields

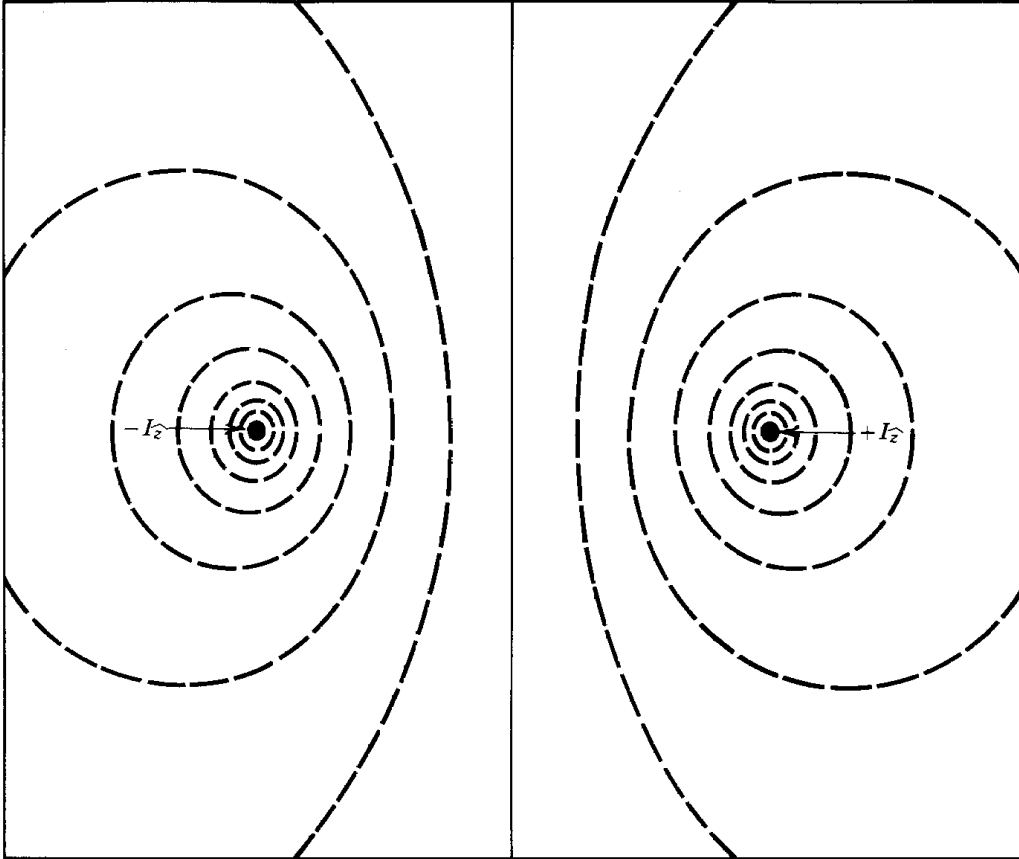


Figure 4.21 Lines of constant vector potential A_z from two wires of infinite extent in z (out of page) carrying equal and opposite currents.

There are many instances in accelerator applications in which magnetic fields are produced by azimuthal currents in cylindrically symmetric systems. For instance, the field of a solenoidal lens (Section 6.7) is generated by axicentered current loops of various radii. There is only one nonzero component of the vector potential, A_θ . It can be shown that magnetic field lines follow surfaces of constant $2\pi r A_\theta$. The function $2\pi r A_\theta$ is called the *stream function*. The contribution from many loops can be summed to find a net stream function.

The vector potential of a current loop of radius a (Fig. 4.22) can be found by application of Eq. (3.24). In terms of cylindrical coordinates centered at the loop axis, the current density is

$$j_\theta = I \delta(z') \delta(r' - a). \quad (4.48)$$

Care must be exercised in evaluating the integrals, since Eq. (3.24) holds only for a Cartesian coordinate system. The result is

Steady State Electric and Magnetic Fields

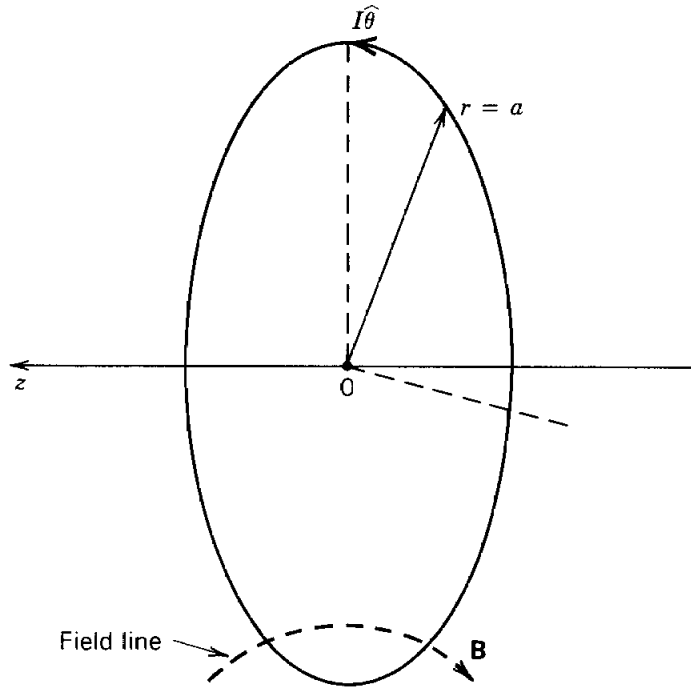


Figure 4.22 Quantities for calculating magnetic fields from a circular current loop.

$$A_{\theta} = \left(\frac{\mu_o I a}{4\pi} \right) \int_0^{2\pi} \frac{\cos\theta' d\theta'}{(a^2 + r^2 + z^2 - 2ar \cos\theta')^{1/2}} . \quad (4.49)$$

Defining the quantity

$$M = 4ar/(a^2 + r^2 + z^2 + 2ar),$$

Eq. (4.49) can be written in terms of the complete elliptic integrals $E(M)$ and $K(M)$ as

$$A_{\theta} = \frac{\mu_o I a}{\pi (a^2 + r^2 + z^2 + 2ar)^{1/2}} \frac{(2-M) K(M) - 2 E(M)}{M} . \quad (4.50)$$

Although the expressions in Eq. (4.50) are relatively complex, the vector potential can be calculated quickly on a computer. Evaluating the elliptic integrals directly is usually ineffective and time consuming. A better approach is to utilize empirical series tabulated in many mathematical handbooks. These series give an accurate approximation in terms of power series

Steady State Electric and Magnetic Fields

and elementary transcendental functions. For example, the elliptic integrals are given to an accuracy of 4×10^{-5} by [adapted from M. Abramowitz and I. A. Stegun, Eds., **Handbook of Mathematical Functions** (Dover, New York, 1970), p. 591].

$$K(M) = 1.38629 + 0.111972(1-M) + 0.0725296(1-M)^2 + [0.50000 + 0.121348(1-M) + 0.0288729(1-M)^2] \ln(1/(1-M)) \quad (4.51)$$

$$E(M) = 1 + 0.463015(1-M) + 0.107781(1-M)^2 + [0.245273(1-M) + 0.0412496(1-M)^2] \ln[1/(1-M)]. \quad (4.52)$$

(4.52)

The vector potential can be calculated for multiple coils by transforming coordinates and then summing A_θ . The transformations are $z \rightarrow (z - z_{cn})$ and $a \rightarrow r_{cn}$, where z_{cn} and r_{cn} are the coordinates of the n th coil. Given the net vector potential, the magnetic fields are

$$B_z = \frac{1}{r} \frac{\partial(rA_\theta)}{\partial r}, \quad B_r = -\frac{\partial A_\theta}{\partial z}. \quad (4.53)$$

A quantity of particular interest for paraxial orbit calculations (Section 7.5) is the longitudinal field magnitude on the axis $B_z(0, z)$. The vector potential for a single coil [Eq. (4.49)] can be expanded for $r \ll a$ as

$$A_\theta(r, z) = \left(\frac{\mu_o I a}{4\pi} \right) \int_0^{2\pi} \left(\frac{\cos\theta' d\theta'}{\sqrt{a^2+z^2}} + \frac{\arccos^2\theta' d\theta'}{\sqrt{a^2+z^2}^3} \right). \quad (4.54)$$

The integral of the first term is zero, while the second term gives

$$A_\theta = \frac{\mu_o I a^2 r}{4 \sqrt{a^2+z^2}^3}. \quad (4.55)$$

Applying Eq. (4.53), the axial field is

$$B_z(0, z) = \frac{\mu_o I a^2}{2 \sqrt{a^2+z^2}^3}. \quad (4.56)$$

Steady State Electric and Magnetic Fields

We can use Eq. (4.56) to derive the geometry of the Helmholtz coil configuration. Assume that two loops with equal current are separated by an axial distance d . A Taylor expansion of the axial field near the axis about the midpoint of the coils gives

$$B_z(0,z) = (B_1+B_2) + (\partial B_1/\partial z + \partial B_2/\partial z) z \\ + (\partial^2 B_1/\partial z^2 + \partial^2 B_2/\partial z^2) z^2 + \dots$$

The subscript 1 refers to the contribution from the coil at $z = -d/2$, while 2 is associated with the coil at $z = +d/2$. The derivatives can be determined from Eq. (4.56). The zero-order components from both coils add. The first derivatives cancel at all values of the coil spacing. At a spacing of $d = a$, the second derivatives also cancel. Thus, field variations near the symmetry point are only on the order of $(z/a)^3$. Two coils with $d = a$ are called Helmholtz coils. They are used when a weak but accurate axial field is required over a region that is small compared to the dimension of the coil. The field magnitude for Helmholtz coils is

$$B_z = \mu_o I / (1.25)^{3/2} a \quad (4.57)$$